Supporting Information (SI) for

Monodisperse Colloidal Gallium Nanoparticles: Synthesis, Low Temperature Crystallization, Surface Plasmon Resonance and Li-Ion Storage

Maksym Yarema,[†‡] Michael Wörle,[†] Marta D. Rossell,[◊] Rolf Erni,[◊] Riccarda Caputo,[†] Loredana Protesescu,[†‡] Kostiantyn V. Kravchyk,[†‡] Dmitry N. Dirin,[†‡] Karla Lienau,[‡] Fabian von Rohr,[†§] Andreas Schilling,[§] Maarten Nachtegaal,[#] and Maksym V. Kovalenko[†‡]*

[†]Laboratory for Inorganic Chemistry, Department of Chemistry, ETH Zürich, Vladimir-Prelog-Weg 1, CH-8093 Zürich, Switzerland;

[‡]Laboratory for Thin Films and Photovoltaics, Empa - Swiss Federal Laboratories for Materials Science and Technology, CH-8600 Dübendorf, Switzerland;

[◊]Electron Microscopy Center, Empa - Swiss Federal Laboratories for Materials Science and Technology, CH-8600 Dübendorf, Switzerland;

[§]Institute of Physics, University of Zürich, CH-8057 Zürich, Switzerland;

[#]Paul Scherrer Institute, CH-5232 Villigen, Switzerland.

[*]Email: mvkovalenko@ethz.ch

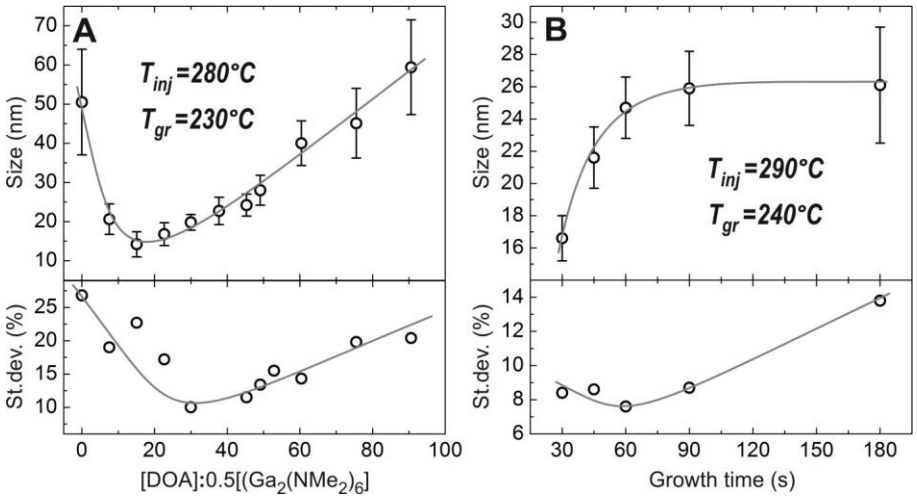

Figure S1. (A) Dependence of the mean size and size-distribution on the amount of added DOA (growth time is 1 min) and (B) as a function of growth time ([DOA]:[Ga] = 30).

Table S1. Experimental conditions for Ga NP syntheses with variable DOA amount (see Figure S1A).

#	ODE, ml	$Ga_2(NMe_2)_6$, mg	DOA, ml	ODE, ml	T_{inj}, °C	T_{growth}, °C	t_{growth}, s	Size, nm	St.dev. %
1	7	25	-	6	280	230	60	50.5±13.5	26.8
2	7	25	**0.28**	5.717	280	230	60	20.6±3.9	19.0
3	7	25	**0.56**	5.435	280	230	60	14.2±3.2	22.7
4	7	25	**0.85**	5.152	280	230	60	16.8±2.9	17.2
5	7	25	**1.13**	4.87	280	230	60	19.8±2.0	10.0
6	7	25	**1.70**	4.305	280	230	60	24.2±2.8	11.5
7	7	25	**1.84**	4.163	280	230	60	28.0±3.8	13.4
8	7	25	**1.98**	4.022	280	230	60	27.3±4.2	15.5
9	7	25	**2.26**	3.74	280	230	60	40.0±5.7	14.3
10	7	25	**2.83**	3.175	280	230	60	45.1±8.9	19.8
11	7	25	**3.39**	2.61	280	230	60	59.4±12.1	20.4

Table S2. Experimental conditions for Ga NP syntheses with variable growth time (see Figure S1B).

#	ODE, ml	$Ga_2(NMe_2)_6$, mg	DOA, ml	ODE, ml	T_{inj}, °C	T_{growth}, °C	t_{growth}, s	Size, nm	St.dev. %
1	7	50	2.26	3.75	290	240	**30**	16.6±1.4	8.4
2	7	50	2.26	3.75	290	240	**45**	21.6±1.9	8.6
3	7	50	2.26	3.75	290	240	**60**	24.7±1.9	7.6
4	7	50	2.26	3.75	290	240	**90**	25.9±2.3	8.7
5	7	50	2.26	3.75	290	240	**180**	26.1±3.6	13.8

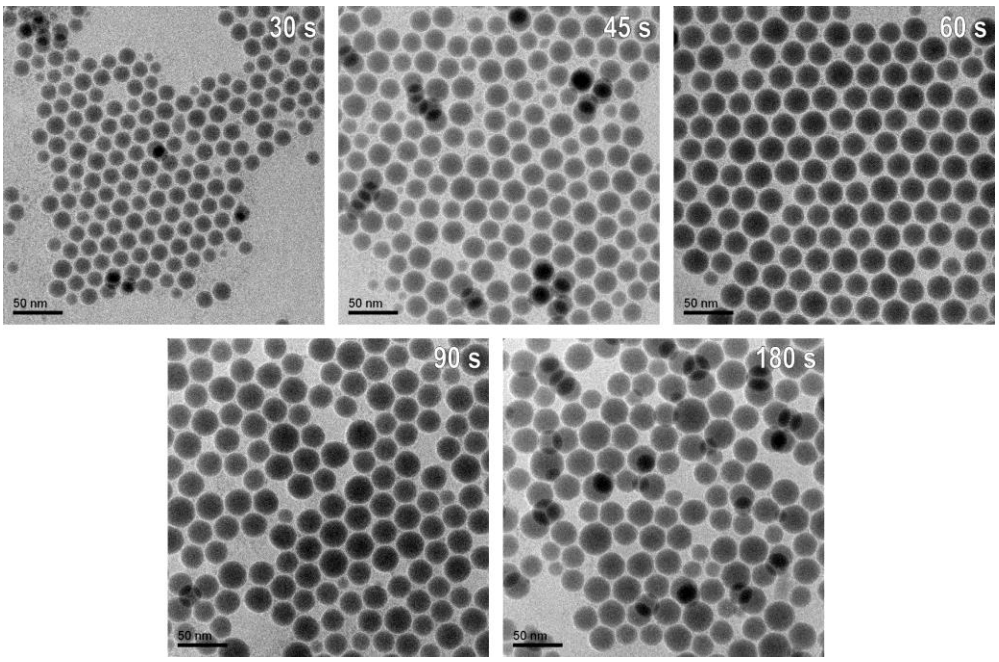

Figure S2. Representative TEM images of the aliquots taken at various growth times ([DOA]:[Ga] = 30, T_{inj} = 290 °C, T_{gr} = 240 °C), indicating an optimal growth time of ca. 1min.

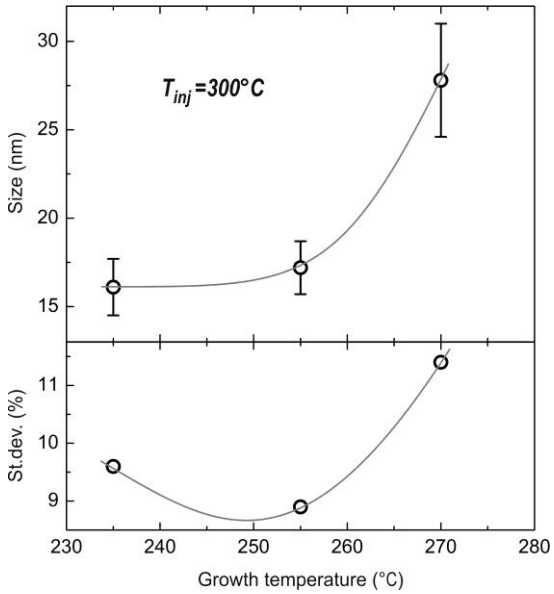

Figure S3. Effect of the difference between the injection and growth temperatures, adjusted by varying the amount of ODE in the injection solution, on the size and size deviation ([DOA]:[Ga] = 30, growth time - 0.5 min).

Table S3. Ga NP syntheses with various differences between the injection and growth temperatures (see Figure S3).

#	ODE, ml	$Ga_2(NMe_2)_6$, mg	DOA, ml	ODE, ml	T_{inj}, °C	T_{growth}, °C	t_{growth}, s	Size, nm	St.dev. %
1	7	25	1.13	**7**	300	**235**	30	16.1±1.6	9.6
2	7	25	1.13	**5**	300	**255**	30	17.2±1.5	8.9
3	7	25	1.13	**3**	300	**270**	30	27.8±3.2	11.4

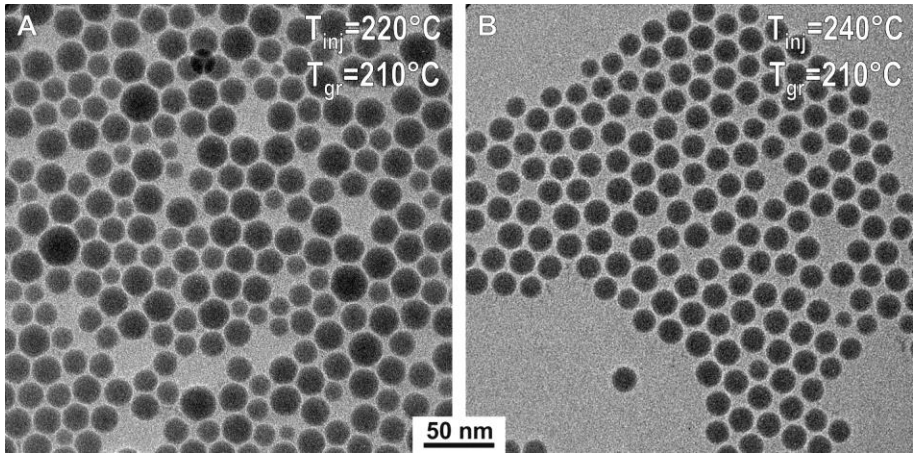

Figure S4. TEM images illustrating the effect of the temperature drop after the injection of gallium precursor on the size distribution ([DOA]:[Ga] = 30, growth time- 1.5 min). The temperature drop is adjusted by the amount of ODE in the injection solution.

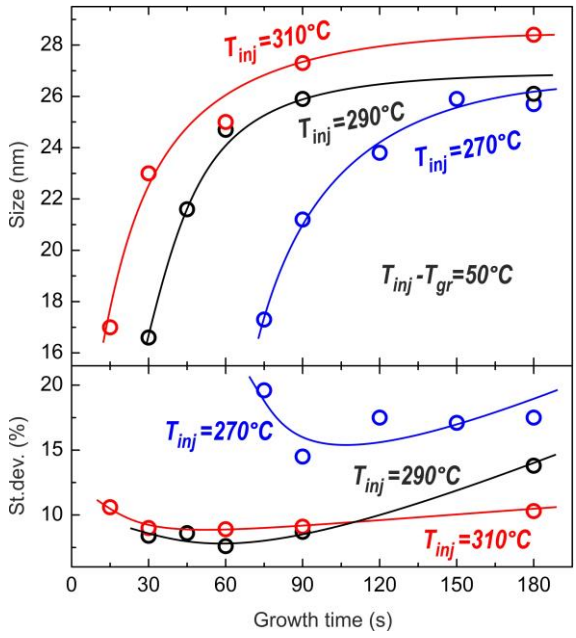

Figure S5. Relationship between the injection/growth temperature, growth time and size for Ga NPs. [DOA]:[Ga] = 30.

Table S4. Experimental conditions for Ga NP syntheses with variable growth time, for 3 different injection temperatures (see Figure S5).

#	ODE, ml	$Ga_2(NMe_2)_6$, mg	DOA, ml	ODE, ml	T_{inj}, °C	T_{growth}, °C	t_{growth}, s	Size, nm	St.dev. %
1	7	50	2.26	3.75	**270**	220	**75**	17.3±3.4	19.6
2	7	50	2.26	3.75	**270**	220	**90**	21.2±3.1	14.5
3	7	50	2.26	3.75	**270**	220	**120**	23.8±4.6	19.5
4	7	50	2.26	3.75	**270**	220	**150**	26.4±3.9	14.6
5	7	50	2.26	3.75	**270**	220	**180**	25.7±4.5	17.5
6	7	50	2.26	3.75	**290**	240	**30**	16.6±1.4	8.4
7	7	50	2.26	3.75	**290**	240	**45**	21.6±1.9	8.6
8	7	50	2.26	3.75	**290**	240	**60**	24.7±1.9	7.6
9	7	50	2.26	3.75	**290**	240	**90**	25.9±2.3	8.7
10	7	50	2.26	3.75	**290**	240	**180**	26.1±3.6	13.8
11	7	50	2.26	3.75	**310**	260	**15**	17.0±1.8	10.6
12	7	50	2.26	3.75	**310**	260	**30**	23.0±2.1	9.0
13	7	50	2.26	3.75	**310**	260	**60**	25.0±2.2	8.9
14	7	50	2.26	3.75	**310**	260	**90**	27.3±2.5	9.1
15	7	50	2.26	3.75	**310**	260	**180**	28.4±2.9	10.3

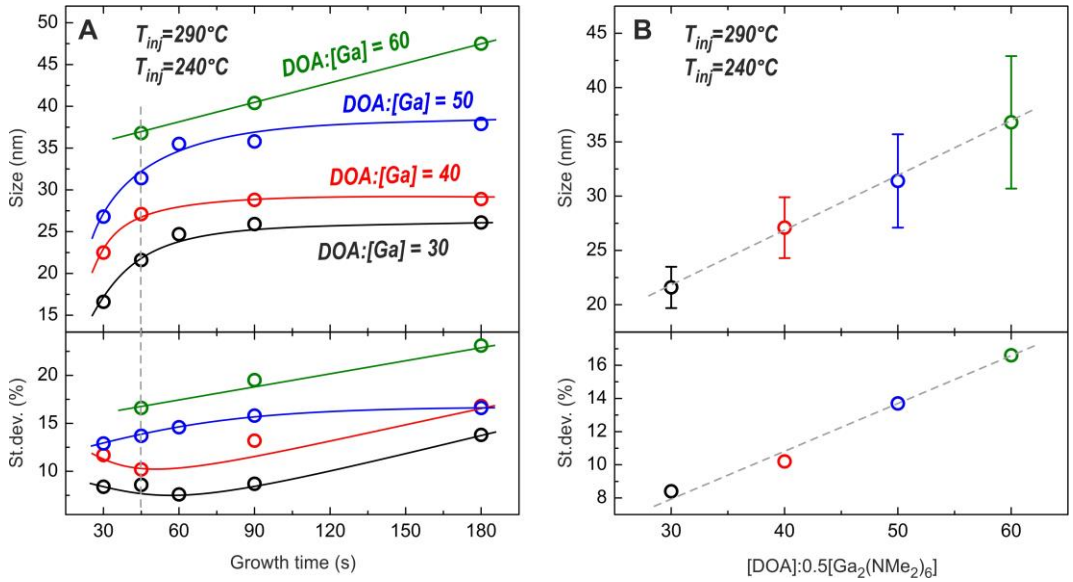

Figure S6. Relationship between the size/size distribution and growth time for various [DOA]:[Ga] molar ratios (same injection and growth temperatures). (B) A slice from A corresponding to the growth time of 45s.

Table S5. Experimental conditions for Ga NP syntheses with variable DOA-to-Ga molar ratios (see Figure S6).

#	ODE, ml	$Ga_2(NMe_2)_6$, mg	DOA, ml	ODE, ml	T_{inj}, °C	T_{growth}, °C	t_{growth}, s	Size, nm	St.dev. %
1	7	50	**2.26**	3.75	290	240	**30**	16.6±1.4	8.4
2	7	50	**2.26**	3.75	290	240	**45**	21.6±1.9	8.6
3	7	50	**2.26**	3.75	290	240	**60**	24.7±1.9	7.6
4	7	50	**2.26**	3.75	290	240	**90**	25.9±2.3	8.7
5	7	50	**2.26**	3.75	290	240	**180**	26.1±3.6	13.8
6	7	50	**3.01**	2.987	290	240	**30**	22.5±2.6	11.7
7	7	50	**3.01**	2.987	290	240	**45**	27.1±2.8	10.2
8	7	50	**3.01**	2.987	290	240	**90**	28.8±3.8	13.2
9	7	50	**3.01**	2.987	290	240	**180**	28.9±4.9	16.8
10	7	50	**3.77**	2.234	290	240	**30**	26.8±3.5	12.9
11	7	50	**3.77**	2.234	290	240	**45**	31.4±4.3	13.7
12	7	50	**3.77**	2.234	290	240	**60**	35.5±5.2	14.6
13	7	50	**3.77**	2.234	290	240	**90**	35.8±5.6	15.8
14	7	50	**3.77**	2.234	290	240	**180**	37.9±6.3	16.6
15	7	50	**4.52**	1.48	290	240	**45**	36.8±6.1	16.6
16	7	50	**4.52**	1.48	290	240	**90**	40.4±7.9	19.5
17	7	50	**4.52**	1.48	290	240	**180**	47.5±11.0	23.1

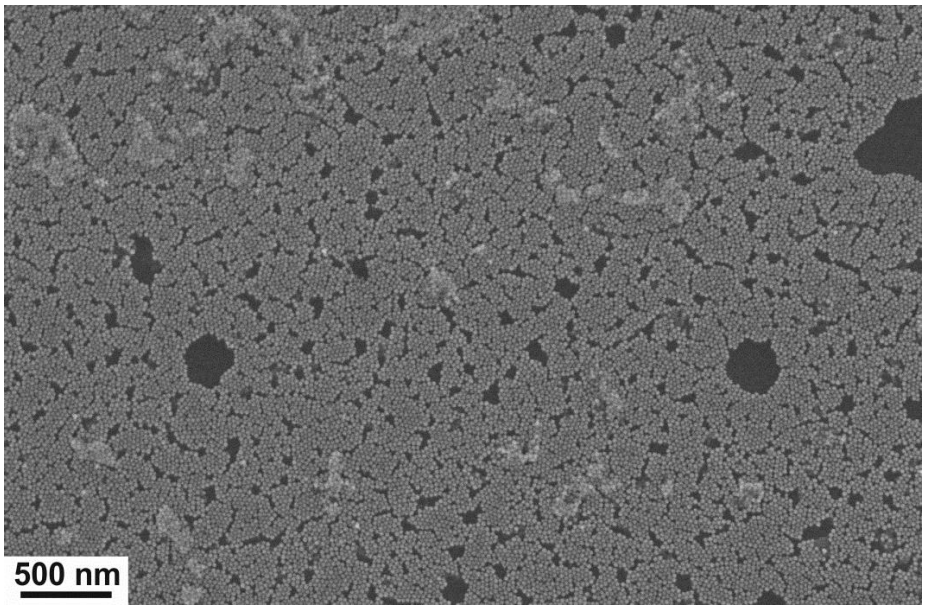

Figure S7. Overview SEM picture of a monolayer of Ga NPs on silicon substrate.

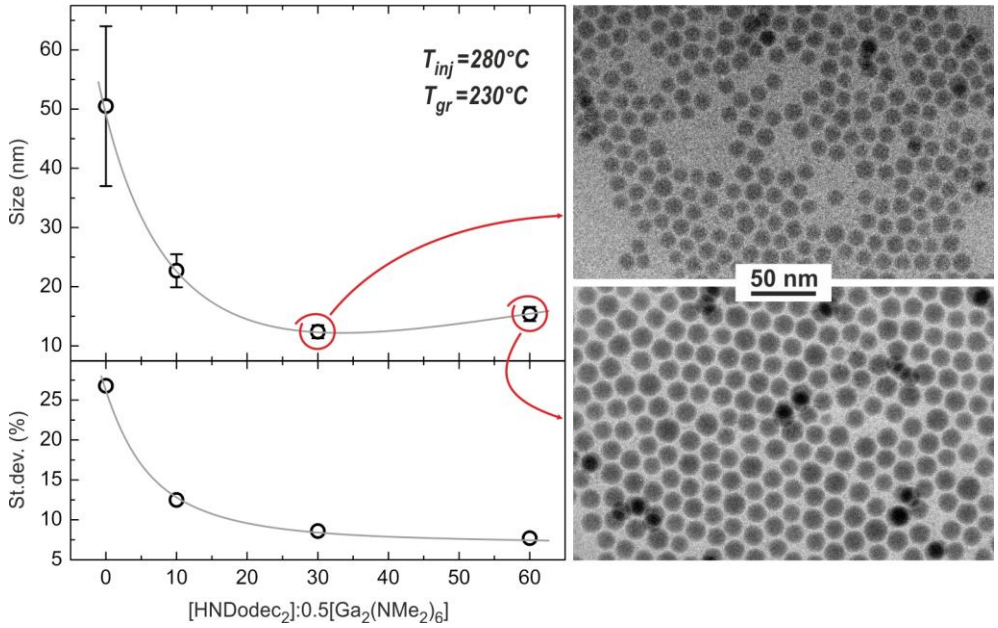

Figure S8. Relationship between the size/size-distribution and the amount of added di-*n*-dodecylamine ($HNDodec_2$). Growth time was 1 minute.

Table S6. Experimental conditions for Ga NP syntheses with variable amounts of di-*n*-dodecylamine in the reaction mixture (see Figure S8).

#	ODE, ml	$Ga_2(NMe_2)_6$, mg	DDA, g	ODE, ml	T_{inj}, °C	T_{growth}, °C	t_{growth}, s	Size, nm	St.dev. %
1	7	25	-	6	280	235	60	50.5±13.5	26.8
2	7	25	**0.44**	5.4	280	230	60	22.7±2.8	12.5
3	7	25	**1.31**	4.2	280	230	60	12.4±1.1	8.6
4	7	25	**2.62**	2.4	280	230	60	15.4±1.2	7.7

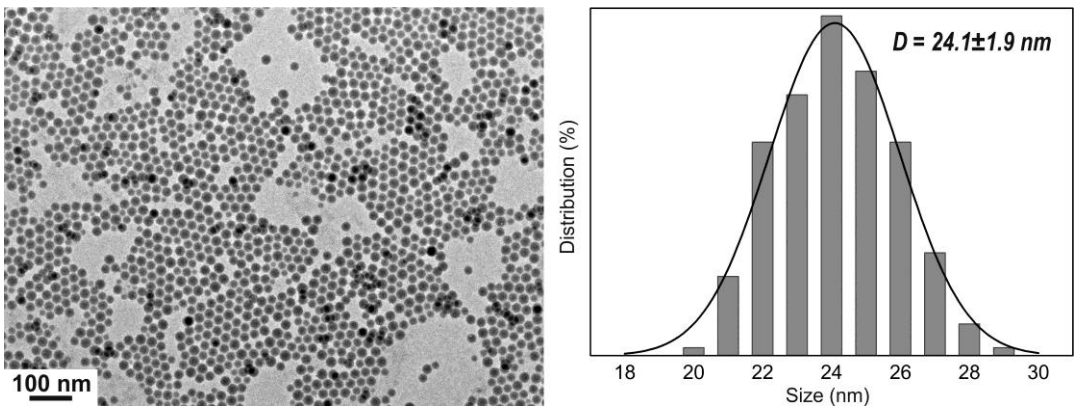

Figure S9. Representative TEM image and a size distribution histogram of the 4×upscaled synthesis of Ga NPs.

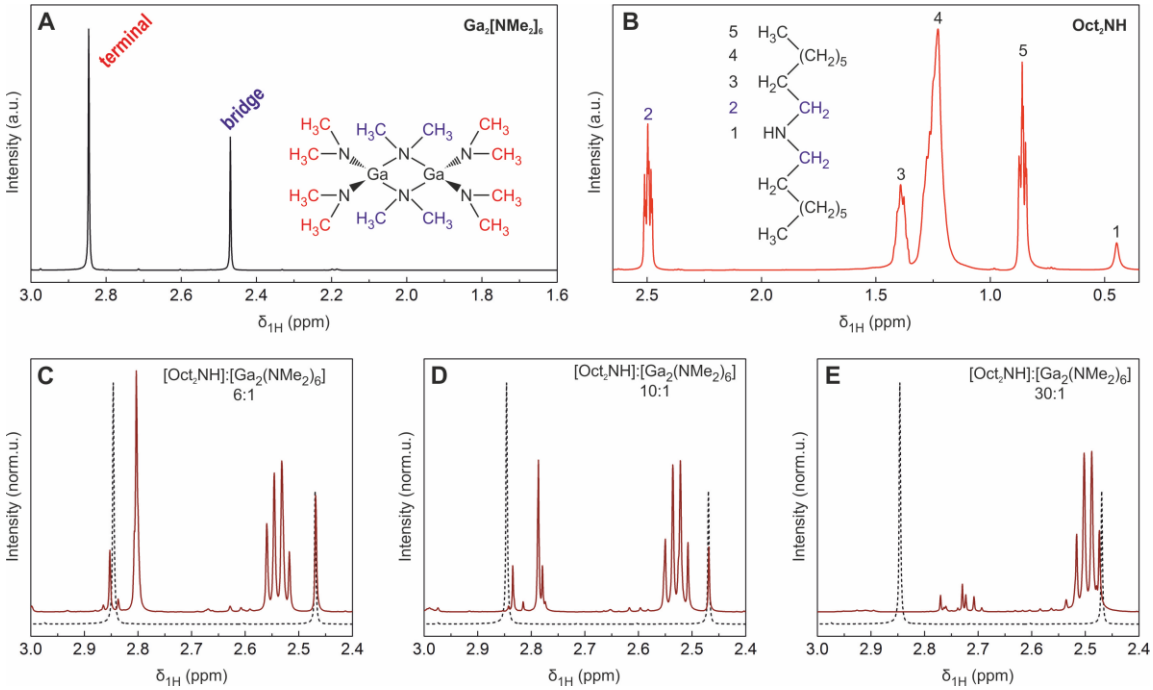

Figure S10. ^{1}H NMR of C_6D_6 solutions of $Ga_2(NMe_2)_6$ (A), DOA (B), and mixtures of $Ga_2(NMe_2)_6$ and DOA with different [DOA]:[$Ga_2(NMe_2)_6$] molar ratios of 6 (C), 10 (D) and 30 (E). The ^{1}H NMR spectrum of $Ga_2(NMe_2)_6$ in (C-E, black dashed line) is given for comparison.

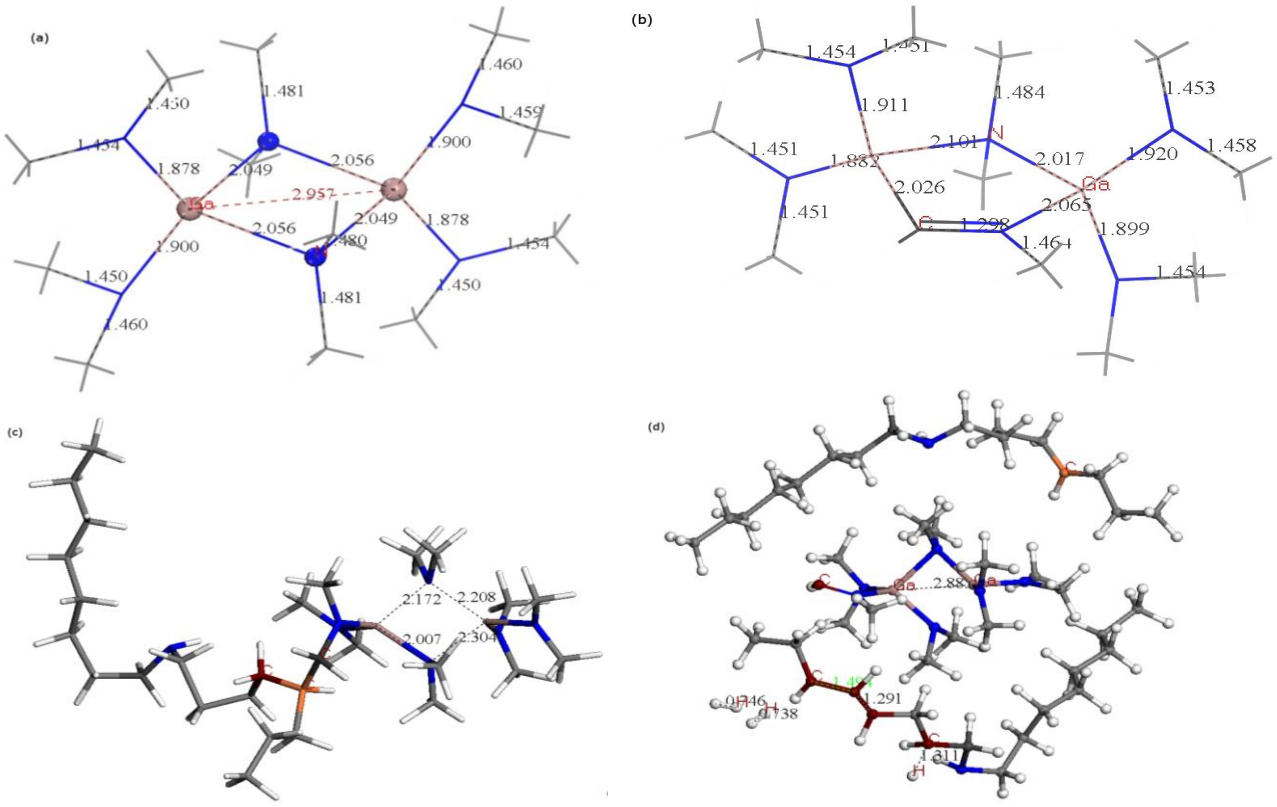

Figure S11. (a) The optimized structure of $Ga_2(NMe_2)_6$ at T = 0. (b) The transition state of $Ga_2(NMe_2)_6$ at 250°C. The H_2 molecule released showed a bond lengths H-H of 0.751 Å. It is cut off the figure. (c) The transition state at 280°C of the system formed by $Ga_2(NMe_2)_6$ and one DOA molecule. The Ga-N(bridging) distances are reported. The carbon atoms participating in the C-H bond cleavage (in orange), the formation of the new C-C bond (C-orange-C-black) and the transfer of the proton (C-dark red) are colored differently. (d) A trajectory at 280°C of the system formed by $Ga_2(NMe_2)_6$ surrounded by two DOA molecules. The C atoms which undergo to C-H bond cleavage are colored in orange (the first) and in brown (the successive ones). Default representing colors: Ga, brown; N, blue; C, black; H, white.

Discussion. The precursor, $Ga_2(NMe_2)_6$, contains square planar conformation of two Ga and two N-bridging atoms. There are two short Ga-N bonds, 1.878 Å and 1.900 Å and two longer Ga-N bonds, 2.049 Å and 2.056 Å, between Ga and the bridging nitrogen atoms and the Ga-Ga distance is 2.957 Å, as shown in Figure S11a. To get an insight into the possible mechanism of the Ga NP formation, we studied the thermal behavior via molecular dynamics simulations at different temperatures for the $Ga_2(NMe_2)_6$ precursor, DOA ligand, and ODE solvent, first as single isolated molecules and then as combined systems. In particular, we considered the isolated $Ga_2(NMe_2)_6$, the system formed by one molecule of $Ga_2(NMe_2)_6$ plus one and two DOA molecules and one $Ga_2(NMe_2)_6$ plus one DOA and one ODE molecules. The molecular dynamics simulations at different temperatures (200 °C, 250 °C, 280 °C, 300 °C, 327 °C) of an isolated $Ga_2(NMe_2)_6$ showed that the thermal decomposition occurs at temperature higher than 200 °C. In fact, at 200 °C the stretching modes of C-H and C-N bonds as well the rotation of the methyl groups along the axis passing through the C-N bonds are activated but the bonds are not broken. The Ga-N(bridging) bonds enlarge up to 2.25 Å. With increasing the temperature the Ga-N(bridging) bonds become loose and the dimer opens. In particular, at 250 °C the two successive C-H

bond cleavages on the same methyl group not only open the dimer but also make possible the formation of a Ga-C bond, while the two released hydrogen atoms can form molecular hydrogen, as shown in Figure S11b. That configuration represents, in fact, a transition state from the $Ga_2(NMe_2)_6$ dimer ground-state to a completely open configuration in which the Ga-N bonds are broken. The C-bridging configuration is also observed at higher temperatures, in particular at 300 °C at which the Ga-N and N-C bonds are more activated and the NMe_2-groups undergo fragmentation and the Ga atoms, getting closer, can start to cluster. Definitely at higher temperatures such as 327 °C $Ga_2(NMe_2)_6$ proceeds to a complete thermal decomposition: the methyl groups losing the hydrogen atoms can recombine to form acetylene molecules, while the hydrogen atoms can form molecular hydrogen. Clearly, the isolated $Ga_2(NMe_2)_6$ cannot provide a complete rationale for understanding the experimental mechanism of reaction, because the ligand and the solvent do participate in the overall reaction. In fact, as the reaction mixture contains an excess of them over the precursor, the molecular dynamics simulations can provide a better insight if they are explicitly considered in the molecular dynamics simulations. The system formed by $Ga_2(NMe_2)_6$ dimer plus one DOA molecule at 280 °C showed that the C-H bond cleavage on the octyl group in DOA and on the methyl group in Ga-DMA leads to the formation of a branched amino ligand to one Ga atom, as shown in Figure S11c. The system formed by $Ga_2(NMe_2)_6$ plus two DOA can mimic the case in which the dimer is diluted and surrounded by DOA only. The molecular dynamics of such a system at T =280 °C showed the C-H bond cleavage on one of four octyl groups as the first decomposition step. Then the C(5)-H is followed by the C(6)-H bond cleavage on the second DOA molecule and C-H bond cleavage on the nearest methyl group on $Ga_2(NMe_2)_6$. The Ga-N(bridging) bond lengths get larger (2.26 Å and 2.15 Å) and the Ga-Ga distance shorter (2.89 Å). Molecular hydrogen can be formed. Successive C-H bond cleavages occur on the octyl group closer to the methyl group from which H atoms have been released: C(2)-H, C(4)-H, C(5)-H and C(6)-H, as shown in Figure S 11d. The molecular dynamics at 280 °C of the system formed by $Ga_2(NMe_2)_6$ surrounded by one DOA and one ODE molecules showed that the first C-H bond to be activated and eventually broken is on the octyl ligand. In fact, the C(5)-H bond on one of the octyl ligands is broken, followed by the C-H bond cleavage on the nearest methyl group on the Ga-DMA. The hydrogen released from the methyl group finally binds to the nearest nitrogen atom forming a DMA molecule. The Ga-N bond lengths enlarged. Even in its drastic simplification the molecular dynamics of such a system points out to a reduced reactivity of $Ga_2(NMe_2)_6$ when it is surrounded by one DOA and one ODE. Instead, the thermal decomposition processes are enhanced and promoted when only DOA molecules surround the precursor. For comparison, we considered the thermal behavior of the $Ga(NOct_2)$, a plausible product of transamination reaction, as suggested by the NMR experiments. The molecular dynamics at 250 °C and 300 °C showed tangles of the long chains and the cleavage of the C-H bonds on the C(8)-H and C(6)-H sites on two octyl groups. The Ga-N bond lengths slightly changed due to the thermal vibration. Only temperature as high as 327 °C the C(1)-H bond cleavage preceded the subsequent Ga-N bond cleavage, because it makes possible the formation of N=C(H) and the detachment of the remaining group.

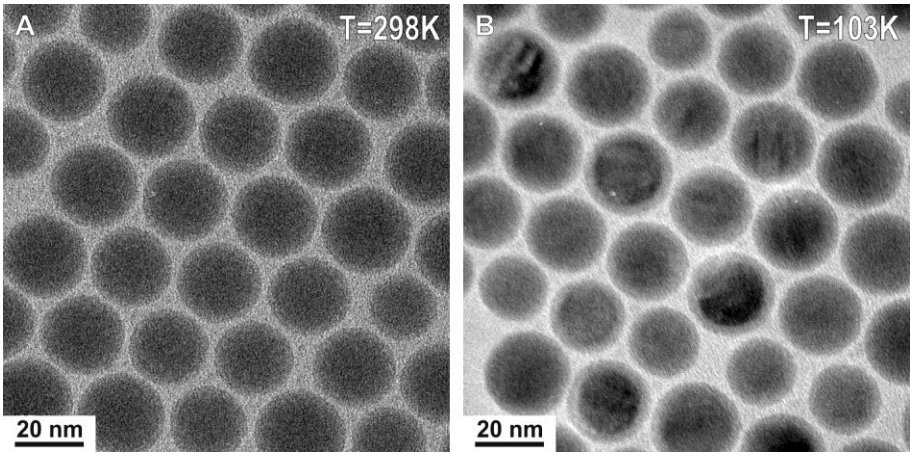

Figure S12. Representative TEM images of Ga NPs measured at room temperature (A) and at 103 K (B). Note the diffraction contrast in (B) due to random orientation of Ga crystallites with respect to the electron beam.

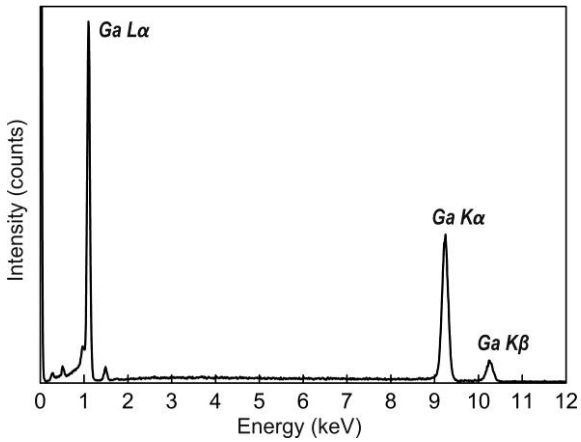

Figure S13. Energy dispersive X-ray (EDX) spectrum of thick Ga NPs film.

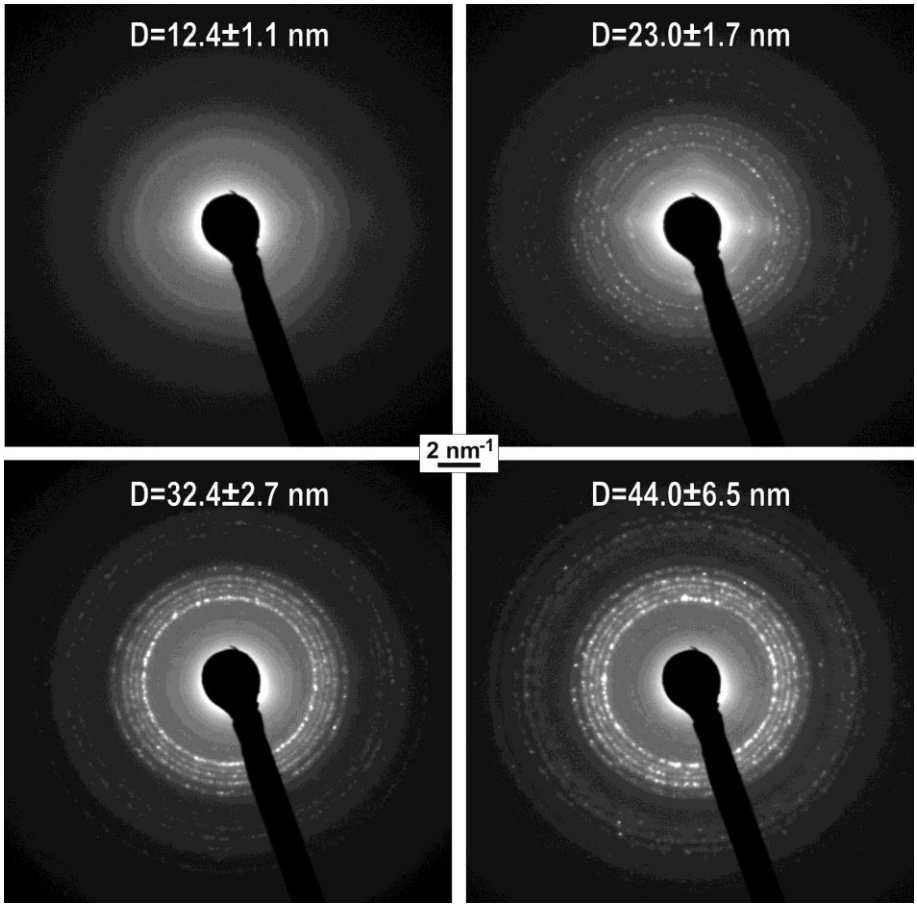

Figure S14. 103K electron diffraction patterns of Ga NPs of 4 sizes.

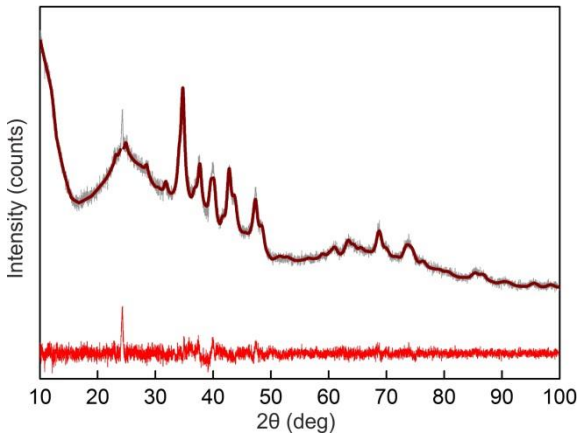

Figure S15. An X-ray diffraction pattern of 24 nm Ga NPs (Cu Kα1, T = 113 K) presented with fitted pattern and difference plot obtained by Rietveld refinement using FullProf Suite software. The weighted pattern and profile R-factors, Rwp and Rp, were 3.72 and 2.91, respectively. The goodness-of-fit indicator (S) was 1.29.

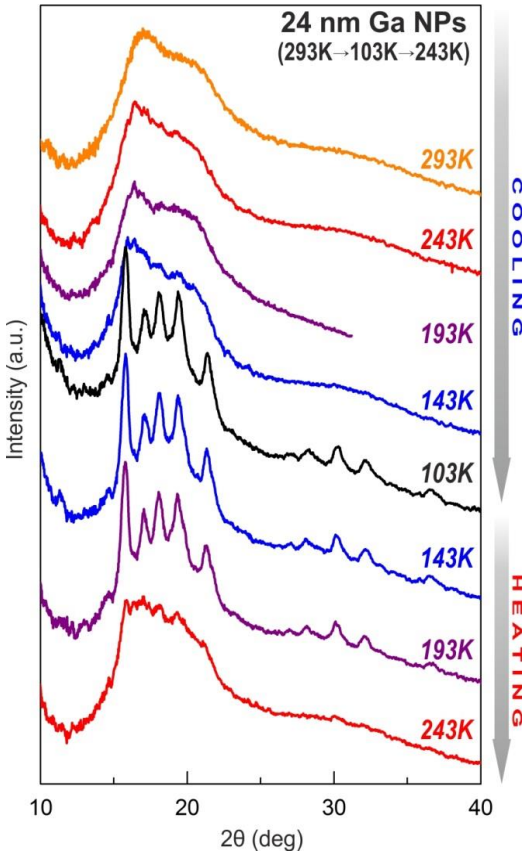

Figure S16. Temperature dependent X-ray diffraction (Mo Kα) of 24 nm Ga NPs during the cooling-heating cycling in the temperature range of 103-293 K.

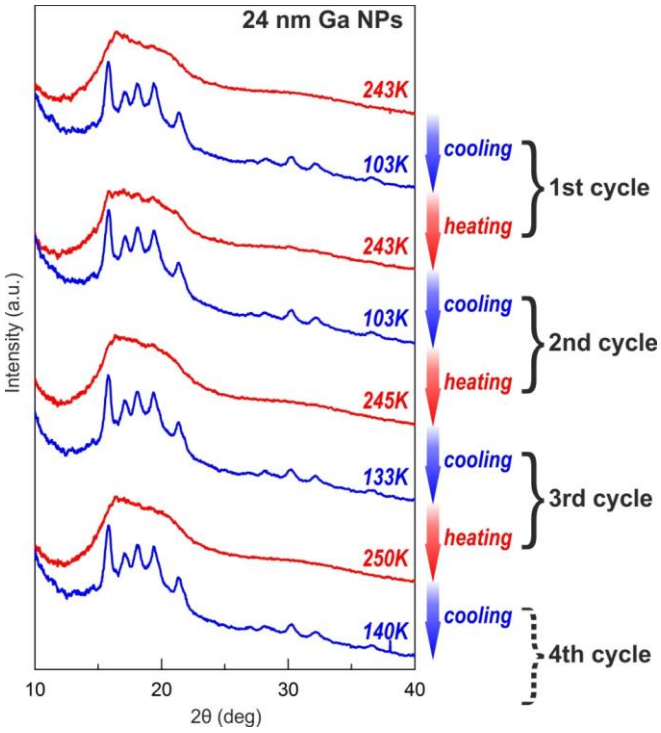

Figure S17. Selected XRD patterns (Mo Kα) for 24 nm Ga NPs showing reversibility of the crystallization and melting. The main crystallite size is retained during thermal cycling.

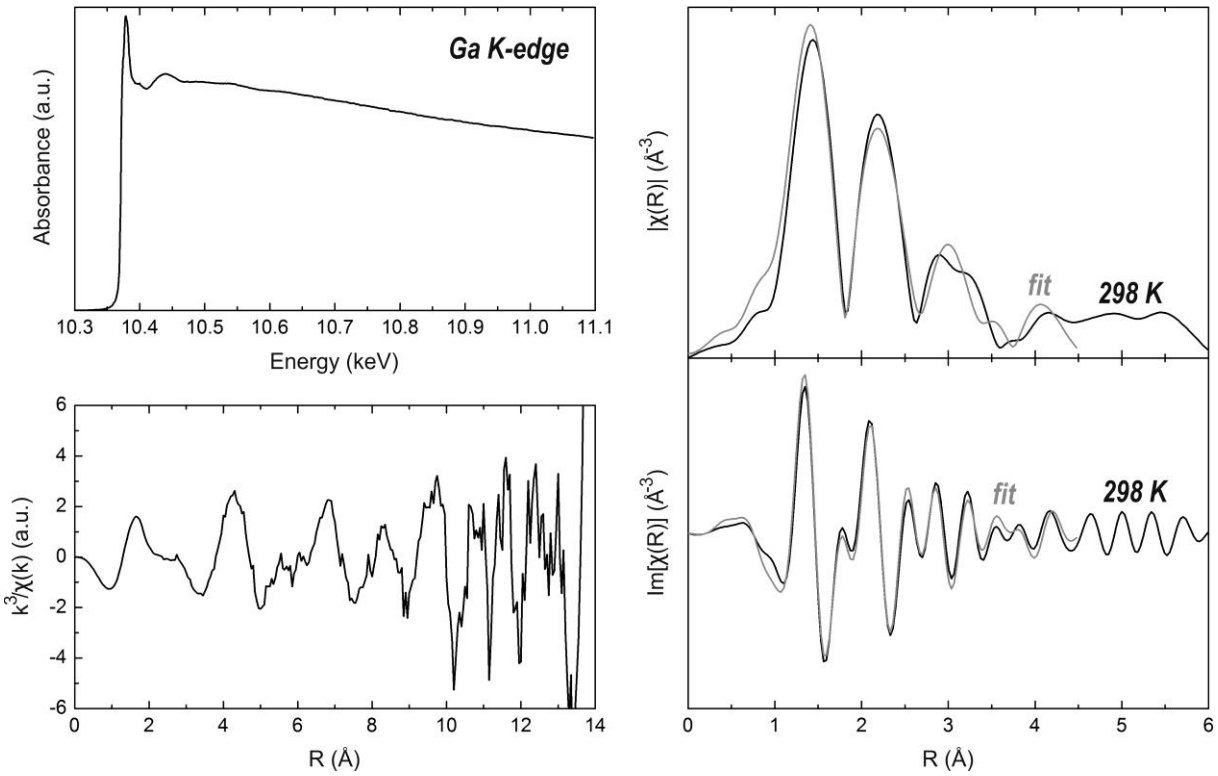

Figure S18. Ga K-edge EXAFS spectrum of 24 nm Ga NPs and radial distribution function (magnitude and imaginary part) for the T = 298 K.

Table S7. Best fit parameters (bond distances, R, and pseudo Debye Waller factors, σ^2) for the EXAFS spectrum taken at 298 K (Figure S18). S_0^2 is the amplitude reduction factor, ΔE_0 is an energy shift between model and data, x is a contribution of oxide phase to the spectrum.

Scattering path	Coordination number	R, Å	σ^2, Å^2
Ga structure			
Ga-Ga	1	2.38 ± 0.02	0.014 ± 0.003
Ga-Ga	6	2.633 ± 0.007	0.018 ± 0.001
Ga-Ga	8	4.02 ± 0.02	0.021 ± 0.003
Ga-Ga	9	4.25 ± 0.02	0.019 ± 0.003
Ga_2O_3 structure			
Ga-O	5	1.863 ± 0.005	0.0001 ± 0.0006
Ga-Ga	11	3.343 ± 0.009	0.007 ± 0.001
Ga-O	10	3.52 ± 0.05	0.009 ± 0.007

$S_0^2 = 0.94 \pm 0.04$

ΔE_0 (Ga) = -2.0 ± 0.7 eV

ΔE_0 (Ga_2O_3) = 2.4 ± 0.7 eV

$x = 0.172 \pm 0.009$

R-factor for this data set is 0.02268

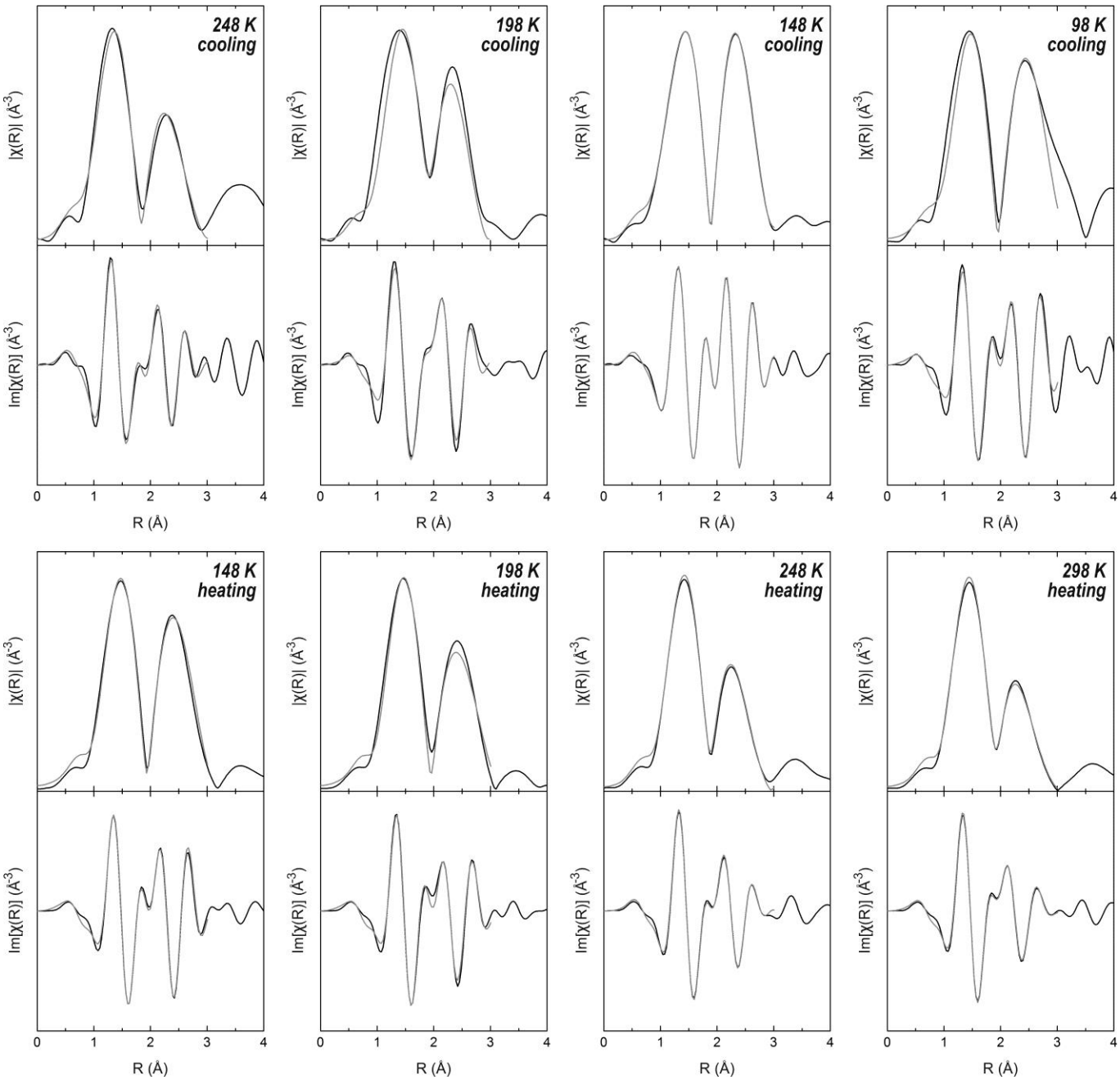

Figure S19. Radial distribution functions (magnitude and imaginary part, black) and a best fit (gray) of EXAFS spectra for 24 nm Ga nanoparticles collected at the Ga K-edge during the cooling-heating scan over the temperature range of 98-298 K.

Table S8. Best fit parameters for the EXAFS spectra taken on Ga K-edge during the cooling-heating scan over the temperature range of 98-298 K (Figures S19). The fraction of oxide, x, is kept fixed to 0.172 as determined at room temperature (Table S7).

T, K	S_0^2	ΔE_0 (Ga), eV	ΔE_0 (Ga_2O_3), eV	R_1 (Ga-Ga), Å	σ_1^2 (Ga-Ga), $Å^2$	R_2 (Ga-Ga), Å	σ_2^2 (Ga-Ga), $Å^2$	R (Ga-O), Å	σ^2 (Ga-O), $Å^2$	R
248 (cooling)	0.92 ± 0.09	-1.8 ± 1.9	1.9 ± 1.8	2.421 ± 0.052	0.0159 ± 0.0059	2.666 ± 0.011	0.0159 ± 0.0016	1.846 ± 0.010	0.0036 ± 0.0016	0.0533
198 (cooling)	0.94 ± 0.06	-9.4 ± 1.1	8.4 ± 1.0	2.387 ± 0.014	0.0069 ± 0.0008	2.628 ± 0.010	0.0183 ± 0.0006	1.881 ± 0.008	0.0024 ± 0.0010	0.0266
148 (cooling)	0.94 ± 0.02	-5.5 ± 0.3	3.0 ± 0.6	2.357 ± 0.003	0.0049 ± 0.0003	2.641 ± 0.002	0.0157 ± 0.0003	1.845 ± 0.003	0.0021 ± 0.0004	0.0022
98 (cooling)	0.96 ± 0.04	3.4 ± 0.8	9.7 ± 0.9	2.544 ± 0.018	0.0190 ± 0.0026	2.789 ± 0.013	0.0206 ± 0.0007	1.918 ± 0.007	0.0036 ± 0.0008	0.0109
148 (heating)	0.88 ± 0.02	3.4 ± 0.4	9.2 ± 0.5	2.523 ± 0.010	0.0172 ± 0.0014	2.758 ± 0.005	0.0186 ± 0.0008	1.922 ± 0.003	0.0004 ± 0.0003	0.0044
198 (heating)	0.89 ± 0.04	4.1 ± 0.9	9.4 ± 0.9	2.557 ± 0.026	0.0209 ± 0.0036	2.779 ± 0.015	0.0221 ± 0.0008	1.918 ± 0.006	0.0007 ± 0.0006	0.0167
248 (heating)	0.98 ± 0.04	-6.4 ± 0.9	5.4 ± 0.8	2.349 ± 0.010	0.0151 ± 0.0021	2.619 ± 0.009	0.0227 ± 0.0011	1.878 ± 0.006	0.0007 ± 0.0005	0.0105
298 (heating)	0.98 ± 0.02	-3.0 ± 0.6	7.1 ± 0.4	2.406 ± 0.010	0.0227 ± 0.0031	2.662 ± 0.008	0.0264 ± 0.0010	1.895 ± 0.003	0.0004 ± 0.0003	0.0023

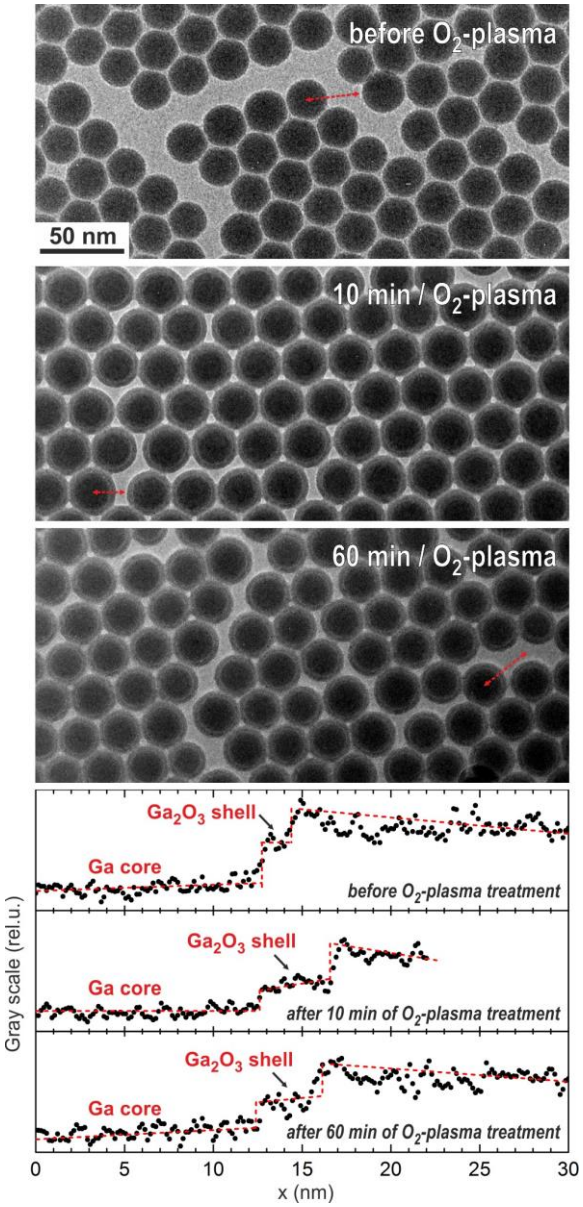

Figure S20. Representative TEM images and gray scale intensity line profiles of Ga NPs before and after O_2-plasma treatment.

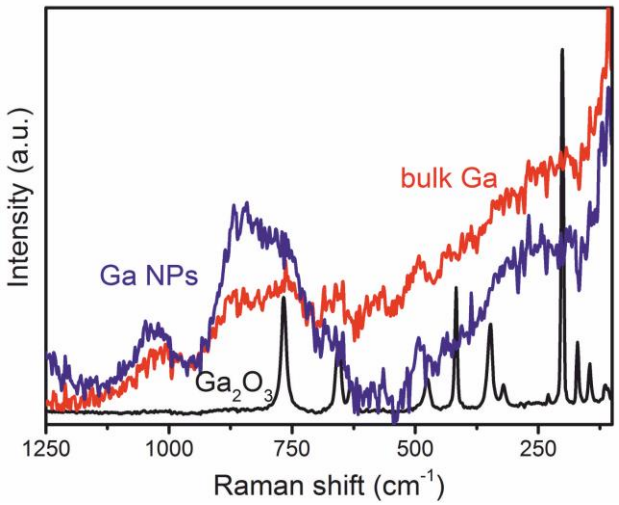

Figure S21. Raman spectra (Thermo Fisher DXR Raman microscope, 455 nm laser for excitation) for Ga NPs and reference samples of bulk Ga and β-Ga_2O_3.